The latest version is at http://www.jbc.org/cgi/doi/10.1074/jbc.M110.205328

Peptide-Protein interactions Suggest that Acetylation of Lysines 381 and 382 of p53 is important for Positive Coactivator 4/p53 Interaction

Subrata Debnath[1], Snehajyoti Chatterjee[2], Mohammed Arif[2], Tapas K. Kundu[2] and Siddhartha Roy[1]

[1]Division of Structural Biology and Bioinformatics, Indian Institute of Chemical Biology, CSIR, 4, Raja S.C. Mullick Road, Kolkata-700032, India

[2]Transcription and Disease Laboratory, Molecular Biology & Genetics Unit, Jawaharlal Nehru Centre for Advanced Scientific Research, Jakkur, Bangalore 560064, India

Running Head: Acetylation of p53 enhances interaction with PC4

Address correspondence to: Siddhartha Roy, Division of Structural Biology and Bioinformatics, Indian Institute of Chemical Biology, CSIR, 4, Raja S.C. Mullick Road, Kolkata-700032, India; Email: sidroykolkata@gmail.com OR

Tapas Kundu, Transcription and Disease Laboratory, Molecular Biology & Genetics Unit, Jawaharlal Nehru Centre for Advanced Scientific Research, Jakkur, Bangalore 560064, India; Email: tapas@jncasr.ac.in

The Human transcriptional positive coactivator 4 or PC4 activates several p53 dependent genes. It has been demonstrated that this is a consequence of direct interaction with p53. Previously, we have concluded that PC4 interacts mainly with the C-terminal negative regulatory domain of p53 through its DNA binding C-terminal half. NMR chemical shift perturbation studies with peptide fragments indicated that amino acids 380-386 of p53 are crucial for interaction with PC4. This was verified by fluorescence anisotropy and sedimentation velocity studies. A peptide consisting of p53 (380-386) sequence, when attached to a cell penetration tag and nuclear localization signal, localizes to the nucleus and inhibits luciferase gene expression from a transfected plasmid carrying a Luc gene under a p53 dependent promoter. Acetylation of lysine-382/381 enhanced the binding of this peptide to PC4 by about an order of magnitude. NMR and mutagenesis studies indicated that Serine-73 of PC4 is an important residue for recognition of p53. Intermolecular nuclear Overhauser effect placed aspartate-76 in the vicinity of lysine-381, indicating that the region around residues 73-76 of PC4 is important for p53 recognition. We conclude that the 380-386 region of p53 interacts with the region around residues 73-76 of PC4 and acetylation of lysine-382/381 of p53 may play an important role in modulating p53-PC4 interaction and as a consequence PC4 mediated activation of p53 target genes.

p53 is a well known tumor suppressor which is essential for cellular integrity and homeostasis. Under normal conditions, p53 is a very short lived protein and in normal cells it is present in low amounts; upon genotoxic insult like DNA damage, hypoxia, expression or over-expression of oncogenes and nucleotide deprivation the levels of p53 is elevated as it is stabilized by various factors. Several post-

translational modifications (acetylation, phosphorylation, methylation, ubiquitination and sumoylation) regulate p53 activation and stabilization (1). p53 is regulated by diverse pathways and has many interacting partners. Various interacting partners of p53 positively or negatively regulate its stability and function. For example, MDM2, COP I and PirH2 negatively regulate p53 by promoting its ubiquitination, whereas p19ARF and HAUSP positively regulate p53 function by preventing MDM2-p53 interaction and enhance deubiquitination (2-7). Lesser number of proteins is known which directly interact with p53 and positively regulate its functions without modifying the p53-MDM2 interactions. Some of these proteins are highly abundant nuclear proteins often associated with chromatin. These include the High-mobility-group protein B1 (HMGB1)(8) and PC4.

PC4 is a multifunctional, highly abundant nuclear protein originally discovered as a transcriptional coactivator that activates activator-dependent DNA transcription through RNA polymerase II (9). It plays crucial roles in transcription, replication, DNA repair, and normal cellular growth. PC4 stimulates ligase-mediated DNA end joining thus acting as an activator of non-homologous end joining and DSB repair activity (10). It binds non-specifically to single and double stranded DNA (11,12). The dsDNA binding ability of PC4 is essential for its coactivator function. Recently, it has been shown to be a bona fide non-histone component of chromatin which plays important role in chromatin compaction and plays a crucial role in maintaining the dynamic chromatin organization, and heterochromatin gene silencing. It is present in all stages of cell cycle (13,14). Mechanistically, PC4 directly interacts with p53 through its C-terminal domain as well as DNA binding domain and enhances DNA binding of p53 to its cognate sites which induce p53 driven transcription and thereby apoptosis (15,16). Although, interaction of PC4 and p53 is critical for PC4 mediated activation of p53 function, PC4 assisted DNA bending also significantly contributes in the enhancement of DNA binding of p53 as well as its downstream function.

PC4 is subjected to various posttranslational modifications. It gets acetylated by another coactivator, p300 and phosphorylated by casein kinase II. Acetylation enhances its dsDNA binding ability. Interestingly, phosphorylation of PC4 inhibits acetylation by p300 and hence, its double stranded DNA binding ability (9,16,17). However, little is known about how p53 post-translational modifications affect p53-PC4 interaction. Recently, it has been discovered that PC4 is a p53 responsive gene, which established the first known positive loop in the regulation of p53 function (18). If post-translational modifications of p53 affect p53-PC4 interaction, it may indicate presence of other regulatory networks, preceding gene expression. In order to first understand the mechanism of PC4 and p53 interaction from a structure-function perspective, and its correlation with the downstream effect in PC4 mediated activation of p53 function, we have investigated the structural components involved in the PC4-p53 interaction by employing NMR spectroscopy and other biophysical techniques. We have employed synthetic peptides corresponding to various parts of the C-terminal region extensively. Since it is difficult and perhaps impossible to obtain the whole protein with defined acetylations, peptide models are only approach to study the effect of acetylation. Similar approaches have yielded important results for phosphorylation dependent effects (19). This approach is better suited

for this region of p53 as it is likely to be not part of a distinctly folded domain. Although the indicative results in some cases were obtained from peptide models, the results have been validated through different functional experiments. This clearly suggests that specific amino acid residues of PC4 interacts with a very specific domain of p53 resulting in the downstream effects. Importantly, we identify a crucial acetylation that enhances p53-PC4 interaction.

Experimental Procedure

Materials----Ni-NTA Sepharose, Heparin-Sepharose, Glutathione-Sepharose, Benzamidine-Sepharose, SP-Sepharose and pre-packed FPLC columns Superdex-75 were from GE Healthcare. PMSF was from Sigma Chemical Company (St. Louis, MO, USA). Reduced glutathione was from JT Baker. $^{15}NH_4Cl$ and d_5-Glycine were from Cambridge Isotope Laboratory. 5(6)-carboxy-fluorescein was from Novabiochem. Thrombin was from GE Healthcare. T4 Polynucleotide Kinase was from Bangalore Genei. All other chemicals used were of analytical grade.

Site-directed mutagenesis----The point mutants of PC4-His_6, PC4S73A and PC4Q65A, point mutant of FLAG tagged PC4, PC4S73A and PC4Q65A, point mutant of GST p53, p53K381A, p53K382A, p53L383A and p53H387A were made by the site-directed mutagenesis technique (QuikChange II XL site-directed mutagenesis kit; Stratagene) as per the manufacturer's instructions. Mutants were confirmed by sequencing. Expression and purification of the mutant proteins were carried out as described for wild type proteins below.

Purification of proteins----For NMR and other biophysical experiments the protein was purified according to following protocol. The pET28b plasmid encoding the protein was transformed in BL21(DE3) and the cells were grown in Luria broth containing 25 μg/ml of kanamycin at 37^0C at 180 rpm until the A_{600} reached 0.5-0.6. For PC4 the cells were induced with 0.7 mM IPTG at 37ºC for 3 h. Cells were harvested by centrifugation. The harvested cells were re-suspended in 20 mM Tris-HCl buffer, pH 7.4 containing 200 mM KCl, 25 mM imidazole, 5 mM β-Me, 10% glycerol and 1 mM PMSF. Cells were sonicated on ice and the lysate was cleared by centrifugation (14,000 rpm, 30 min, 4°C). Affinity chromatographic purification of this protein was done using Ni-NTA Sepharose column. The pooled fractions from the Ni-NTA column was dialyzed against BC200 buffer (20 mM Tris-HCl buffer, pH 7.4 containing 200 mM KCl, 0.2 mM EDTA, 10 mM β-Me and 10% glycerol). The protein was then loaded onto Heparin-sepharose column which was pre-equilibrated with BC200 buffer. The column was subsequently washed with BC200 buffer and the protein was eluted by BC400 buffer (20 mM Tris-HCl buffer, pH 7.4 containing 400 mM KCl, 0.2 mM EDTA, 10 mM βMe and 10% glycerol). The protein was then concentrated by polyethylene glycol 20000, dialyzed against 20 mM Tris-HCl buffer, pH 7.4 containing 200 mM KCl, 0.2 mM EDTA, 10 mM β-ME and 10% glycerol. Gel filtration was done on Superdex-75 in FPLC (only for preparation of NMR sample). The purity of the protein was checked by SDS-PAGE followed by Coomassie blue staining. Concentration of the protein was determined by BCA protein assay**.** For the purification of ^{15}N labeled PC4 the same protocol was followed except first cells were grown in LB

medium then transferred to M9 medium containing $^{15}NH_4Cl$.

For GST pull-down and other functional assays, the following protocol was used. Full-length PC4 and its point mutants were purified by Ni-NTA affinity chromatography followed by Heparin-Sepharose affinity chromatography. The proteins, expressed and purified from bacteria, were analyzed on 12% SDS-PAGE and visualized with Coomassie staining and confirmed by immunoblotting using PC4 antibody. FLAG-tagged p53 was bacterially expressed and purified using M2-agarose immunoaffinity chromatography. GST-p53 and its point mutants were expressed and purified using Glutathione Sepharose affinity chromatography.

GST pull-down assay----GST pull-down assays were performed as described previously (15). Briefly, 1 µg of GST, GST-p53, or GST-p53 point mutants bound to Glutathione Sepharose beads were incubated with bacterial lysate containing 200 ng of PC4 or its point mutants in a reaction mixture of 200 µl BC150 buffer (20 mM Tris HCl, pH 7.4 containing 20% glycerol, 0.2 mM EDTA and 0.1% NP-40) containing 150 mM KCl at 4°C for 3 h. The beads were then washed five times with BC150 and were run on 12% SDS-PAGE gels, followed by immunoblotting with PC4 antibody.

Elecrophoretic Mobility Shift Assay (EMSA)---A 36-mer oligonucleotide containing p53 binding sites (5'-TATGCCACGCCCAGGCTTGTCTCTAA CTTGTGAGCC-3') derived from the Bax promoter was labeled by using T4 polynucleotide kinase. The radiolabeled strand was annealed with the complementary strand, and an EMSA was performed as described previously (16). Briefly, 3 ng of radiolabeled probe was incubated in a reaction volume of 40 µl containing 8 µl of 5X EMSA buffer (100 mM HEPES buffer, pH 7.9 containing 125 mM KCl, 0.5 mM EDTA, 50% glycerol and 10 mM $MgCl_2$), 2 µl of 60-µg/ml double-stranded poly dI-dC, 4 µl of bovine serum albumin (BSA) (1 mg/ml) and 2µl of 10 mM DTT with the proteins as indicated for 30 minutes at 30°C. The samples were analyzed on 5% native PAGE in 0.5X Tris-Borate-EDTA buffer, pH 8.0 containing 0.05% NP-40 and electrophoresed at 4°C for 2 hours (200V). The gels were dried and DNA-protein complexes were visualized by PhosphorImage Analyzer (Fuji) using Image Gauge software. Band quantification was done using Phosphor Imager densitometry scanning software.

Luciferase assay----The p53 null human carcinoma cell line H1299 were maintained at 37°C in Dulbecco's modified Eagle medium with 10% fetal bovine serum. The mammalian expression constructs of p53, and PC4 used in this study were placed under a cytomegalovirus (CMV) promoter. The p53-responsive promoter PG13Luc contains 13 consensus p53-binding sites in tandem followed by a polyomavirus promoter, which drives the luciferase gene. This construct was used to monitor the effect of PC4 on p53-mediated gene expression in vivo. The CMV-driven ß-galactosidase (pCMV-ß gal) construct was used as an internal control. Prior to transfection, cells were seeded at 0.6-1 x 10^6 cells per 30-mm-diameter dishes and transfected with different plasmid constructs, using Genejuice (Novagen) according to the manufacturer's protocol. An empty vector was used to keep the total amount of DNA constant in each transfection. Luciferase and ß-galactosidase activities were measured 24 h after the transfection with luciferase assay and ß-galactosidase assay systems according to the procedure provided by manufacturer

(Promega). The transient transfection assay was performed three times independently to monitor average relative luciferase activity (15).

Purification of p53 (364-393)-----The plasmid encoding the protein GST-p53 C-terminal (364-393) was transformed into BL21(DE3) and the cells were grown in Luria broth containing 100 µg/ml of ampicillin at 37°C until A_{600} reached 0.4-0.5. For expression of p53CT, the cells were cooled to 25°C and induced with 1 mM IPTG for 3 h. Cells were harvested by centrifugation. The cell pellet was suspended in 10 mM Tris-HCl buffer, pH 7.5 containing 100 mM KCl, 0.1 mM EDTA, 1% TritonX-100, 5% glycerol and 1 mM PMSF. Cells were sonicated on ice and the lysate was cleared by centrifugation (14,000 rpm, 30 min, 4°C). The supernatant was loaded onto GST-sepharose (GE Healthcare) column which was pre-equilibrated by lysis buffer. The column was washed subsequently with lysis buffer. The GST-tagged fusion protein was eluted by 100 mM Tris-HCl buffer, pH 7.5 containing, 50 mM KCl, 5% glycerol and 20 mM Glutathione. The purified protein was dialyzed against 1X PBS (pH 7.5) and 5% glycerol. Then the protein was digested with thrombin at 22°C, for one and a half hrs and loaded onto benzamidine Sepharose (GE Healthcare) column which was pre-equilibrated by 1X PBS, pH 7.5 containing 5% glycerol for removal of thrombin. The digested protein then was loaded onto SP-sepharose (GE Healthcare) column which was pre-equilibrated with 1 X PBS containing 5% glycerol to remove GST protein. Then the p53 (364-393) protein was eluted by using a 0-1 M KCl gradient in 1XPBS. The eluted fractions were pooled and concentrated by polyethylene glycol 20000, dialyzed against 0.1% acetic acid and purified by HPLC using reverse phase C_{18} column (Hypersil gold, Thermo Fisher) and the mass was checked by ESI (Waters). For the purification of ^{15}N labeled p53 (364-393) the same protocol was followed except first cells were grown in LB medium then transferred to M9 medium containing $^{15}NH_4Cl$.

Peptide synthesis and purification----All peptide nomenclature and corresponding sequences are shown in Table I. All the peptides were synthesized on a 0.1-mmol scale by using a solid-phase peptide synthesis strategy using 9-fluorenylmethoxy carbonyl chemistry and Rink amide MBHA resin. Cleavage of the peptides from Rink amide MBHA resin and removal of all side chain-protecting groups were achieved in 94.5% trifluoroacetic acid, 2.5% water, 2.5% 1, 2 ethanedithiol and 1% triisopropylsilan solution. The crude peptides were purified by reversed-phase high-performance liquid chromatography (Waters Associates) with a C_{18} column (Hypersil gold, Thermo Fisher) with linear gradients of water/acetonitrile containing 0.1% trifluoroacetic acid. Peptides masses and purity (>95%) were checked by ESI (Waters Inc.) and MALDI-Mass spectrometry.

The selectively deuterated peptide was synthesized on 0.1mmole scale by solid phase peptide synthesis strategy using Fmoc chemistry and rink amide MBHA resin. The Lys381 had an ivDde side chain protection group. After the synthesis of the peptide, the N-terminal $–NH_2$ group was cleaved with 20% piperidine and then blocked with Boc using Boc-anhydride. The side chain protecting group ivDde of the Lys381 was then removed with 2% hydrazine and the exposed side chain $–NH_2$ was acetylated with deuterated acetic acid by normal carbodiimide coupling strategy. Finally, the

peptide was cleaved from the resin and removal of all side chain protecting groups were achieved in 94.5% trifluoroacetic acid, 2.5% water, 2.5% 1, 2 ethanedithiol and 1% triisopropylsilan solution. The crude peptide was purified by reversed-phase high-performance liquid chromatography (Waters Associates) with a C_{18} column (Hypersil gold, Thermo Fisher) with linear gradients of water/acetonitrile containing 0.1% trifluoroacetic acid. Peptide mass and purity (>95%) was checked by MALDI-Mass spectrometry.

Peptide labeling----The peptides p53(380-386), p53(380-386, K381A, K382A, L383A), p53(380-386, K381KAc), p53(380-386, K382KAc) and p53(380-386,K386KAc) were labeled with 5,6-carboxy fluorescein in solid phase. Dry resin bound N-terminal deprotected peptide (3 µmole) reacted with 10 times molar excess of 5(6)-carboxy fluorescein, HBTU (1:1) and 20 times molar excess of N-ethyldiisopropylamine in DMF. The reaction was kept for 4 hours in dark at 25^0C. After completion of the reaction, resin was washed thoroughly with 20% piperidine in DMF until the wash solution becomes colorless. Resin was then washed consecutively with DMF and Et_2O for five times and finally dried under N_2 atmosphere. After labeling peptides were cleaved as unlabeled peptides and purified by HPLC and masses were checked by Mass Spectrometer.

NMR spectroscopy----All the NMR experiments were conducted at 37^oC on a 600 MHz Bruker Biospin NMR spectrometer using TCI cryoprobe. The buffer was 50 mM KP, pH 6.2 containing 100 mM KCl. The 1D proton spectra were recorded using the pulse program *zgesgp* and water suppression achieved with excitation sculpting. TOCSY (mixing time 60 ms) spectra were recorded with solvent suppression using WATERGATE and the spinlock in TOCSY experiment was attained by MLEV sequence. The ^{1}H, ^{15}N HSQC spectra were recorded using the pulse program hsqcetfpf3gp with flip back pulses and optimized SP1 with 'gs'. The resonance assignment of PC4 was taken from published data (20).

Edited NOESY----The ^{1}H, ^{15}N isotope-edited NOESY spectra was recorded using the pulse program noesygpphwgx1 with mixing time 400 ms and solvent suppression was achieved using WATERGATE. The isotope-edited NOESY was conducted in 50 mM Potassium phosphate buffer, pH 6.2 containing 50 mM KCl and 50 mM d5 glycine. Reference (21).

Fluorescence anisotropy experiments---- Fluorescence anisotropy measurements were performed at 4^0C by using Quantamaster 6 (PTI) T-geometry fluorometer. The titrations were carried out in 20 mM Tris-HCl buffer, pH 7.4 containing 100 mM KCl, 0.2 mM EDTA, 20% glycerol and 0.1% NP40. Fluorescence anisotropy was measured with excitation at 490 nm and emission at 530 nm using bandwidths of 5 nm on both sides. For competition experiments, the titrations were carried out in same solution conditions as above. 4 nM labeled p53(380-386) peptide was incubated with saturating concentration of PC4 at 4^oC for half an hour and then titrated with unlabeled p53(380-386) and p53(380-386, K381A, K381A, L383A).

Sedimentation velocity----Sedimentation velocity measurements were performed at 4^0C in 20 mM Tris-HCl buffer, pH 7.4 containing 100 mM KCl, 0.2 mM EDTA,

20% glycerol and 0.1% NP40 at the rotor speed 38000 rpm using Beckmann coulter analytical ultracentrifuge (Proteomelab XL-A/XL-I). Scan was recorded at 495 nm and data was fitted dc/dt vs. s* in Origin 6 using sedimentation time derivative analysis. Equations described in the vendor's software package was used. Peptide and protein concentrations were 5 μm each.

Statistical and Computational Methods---- The standard errors were obtained from three or more independent measurements. For fluorescence anisotropy measurements, the binding isotherms were fitted to a single site binding equation:

$$A_{obs} = A_0 + \frac{[(A_\infty - A_0).\{(K_d + X + [pep]) - \sqrt{((K_d + X + [pep])^2 - 4.X.[pep]}\}]}{2[pep]}$$

Where, A_{obs} is the observed anisotropy, A_0 is the initial anisotropy, A_∞ is the final limiting anisotropy, [pep] is the labeled peptide concentration in Molar units, X is the total PC4 concentration and K_d is the dissociation constant in Molar units. The binding model makes no *a priori* assumptions except that there is only one binding site for the p53 peptide per subunit of PC4 and the binding is independent of whether another peptide is bound to the neighboring subunit or not.

Results

In the last few years, PC4 has emerged as an important regulator of many p53 target genes (16). However, little is known about how PC4 mediates the transcription of p53 target genes. In previous articles, it was demonstrated that the C-terminal region (negative regulatory domain) of p53 is most important for this interaction, although the exact mechanism is unclear (16). In order to gain more structural information, we have attempted to identify the amino acids responsible for this interaction.

p53(380-386) region is crucial for interaction with PC4

p53 has a modular structure (22). Figure 1 (*A*) shows the different regions of p53 along with their major functions. Many of these functions are modulated by post-translational modifications. This modular nature often implies that peptides derived from these regions are capable of interacting with partner proteins as well. At first, p53 (364-393) was purified as a GST fusion protein, followed by cleavage and purification of the pure peptide. Chemical shift perturbation was used to identify the possible interacting regions. The whole spectra were difficult to assign and here we focus only on the methyl region of the TOCSY spectra. Figure 1 (*B*) shows the methyl region of the TOCSY spectra of the p53 (364-393) with and without the full-length sub-stoichiometric amount of PC4 and only peptide protons are observable under this conditions. The TOCSY spectra with and without PC4 reveal a number of chemical shift changes; thus, indicating interaction of the peptide and the protein (data not shown). This peptide contains two leucine residues, 369 and 383, and no isoleucine residues, thus making it easier to identify leucine methyl resonances from chemical shift data alone. Of the two leucine methyl peaks in the 0.8-1.0 ppm region in the TOCSY spectra, one shows significant chemical shift change but the other doesn't; clearly indicating that either region around 369 or 383 is responsible for binding to PC4. To identify which region is responsible for PC4 binding, we synthesized two peptides p53 (366-372) and p53 (380-386) and the binding was studied by chemical shift perturbation in the presence or absence

of PC4. Comparison of chemical shifts of methyl protons indicates no significant shift occurs for p53 (366-372) (Figure 1 (*C*)). However, significant chemical shift change is seen for L383 methyl group p53 (380-386), indicating significant interaction of this region with PC4 (Figure 1 (*D*)). This interaction pattern was verified using a GST pull-down assay. The results suggest that the mutation at the lysine 382 residue of p53 substantially reduces its interaction ability with PC4 (Figure 1 (*E*), lane 3 versus lane 5). On the other hand, the effect of mutation at histidine 387 exhibited a moderate level of interaction and the mutation at lysine 381 residue affected the interaction minimally (Figure 1 (*E*), lane 3 versus lane 7 and 4) supporting the conclusion that 380-387 region of p53 is responsible for interaction with PC4 (Figure 1 (*E*)).

We have verified the interaction of this region of p53 with PC4 by two different biophysical techniques: Analytical ultracentrifugation and fluorescence anisotropy. Figure 2 (*A*) and (*B*) show sedimentation velocity profile of fluorescein labeled p53 (380-386) monitored at 495 nm, in the absence and presence of PC4, respectively. The analysis gave a value of Svedberg constant (S_{app}; uncorrected for viscosity and temperature) value of 1.05 not inconsistent with the size of a small peptide. In the presence of PC4, the parent S_{app} peak largely disappears, indicating loss of the free peptide. There are several new species of higher S values. This could be due to peptide bound to different oligomeric states of PC4. The lowest sedimentation value of these different species is 2.95, which most likely originates from the PC4 dimer. The other higher sedimenting species probably are higher order oligomers of PC4. The analytical ultracentrifugation supported the interaction of PC4 with 380-386 region of p53. To obtain a more quantitative measure of the p53-PC4 interaction, we have determined the binding isotherm by fluorescence anisotropy. Figure 2 (*C*) shows the binding isotherm of fluorescein labeled p53 (380-386) with PC4. The binding isotherm shows saturation behavior and when fitted to a single site binding equation it yields a dissociation constant of 2.02 $\pm$ 0.69 nM. From the previous GST pull-down assay it was clear that lysine and leucine residues in this stretch of amino acids probably play a crucial role in the binding, we synthesized a KKL381, 382, 383 AAA-p53 (380-386) peptide. Binding of fluorescein labeled triple alanine substituted peptide with PC4 was monitored by fluorescence anisotropy and the binding isotherm is also shown in Figure 2 (*C*). It is clear from the profile that in contrast to the wild-type peptide, no increase in anisotropy was seen--- indicating that no significant binding occurs in the concentration range studied. Clearly, at least one of the three residues is important for p53 interaction with PC4. In order to confirm that modification of N-terminal end in no way affects the results reported above, we have done competition experiments with the unlabeled peptide. When the PC4 was first allowed to form a complex with Fluorescein labeled p53 (380-386) and then titrated with either unlabeled p53 (380-386) or unlabeled KKL381, 382, 383 AAA p53 (380-386) the anisotropy quickly returns to the free peptide level for the former but stays unchanged for the latter (Figure 2 (*D*)). This clearly indicates that modification of the N-terminal α-amino group has no significant effect on the binding of the peptides.

Acetylation of Lysine 381 and 382 enhances p53-PC4 interaction

It was established previously that acetylation of both PC4 and p53 enhance their interactions. However, little is known

about the identity of the residues that are involved in this interaction. This is important as it is already established that acetylation of different lysine residues in p53 produces different functional outcomes. We have thus used the fluorescence anisotropy technique to study the interaction of p53 (380-386) with PC4 as described before. In these experiments, bacterially produced recombinant PC4 was used and thus assumed to be not post-translationally modified. Figure 3 shows the binding isotherms of p53 (380-386) acetylated in either K381 or K382 or K386, respectively with PC4. The binding isotherm was fitted to a single binding site to yield a dissociation constant of 0.52 $\pm$ 0.18, 0.94 $\pm$ 0.29 and 1.58 $\pm$ 0.36 nM respectively. The error analysis reported here are obtained from 4-5 separate experiments done under identical conditions and statistical analysis was performed from K_ds obtained from individual experiments. This indicates that both K381 and K382 acetylation enhances the binding affinity of p53 (380-386). Figure 3 also shows the binding isotherm of triply acetylated p53 (380-386) [K381, K382, K386] with PC4. The obtained dissociation constant is 0.35 $\pm$ 0.16 nM, which indicates some additive effect. Thus, acetylation of K386 appears to have no role in strengthening interaction with PC4.

p53 (380-386) peptide inhibits p53-PC4 interaction in cell

Since, p53 (380-386) has a high affinity for PC4, it may be possible to direct it to the nucleus and inhibit PC4 mediated activation of p53 target genes. We have thus attached a cell penetration tag to this peptide (hexa D-arginine) and a nuclear localization signal (NLS) and attempted to find out the effect of this peptide to PC4 mediated activation of p53. First, we have attempted to find out if the peptide enters the cell nucleus. N-termini of both the peptides were labeled in the solid phase with fluorescein and the fluorescein modified peptide was used in confocal fluorescence microscopy for localization. Both the peptides are largely concentrated in the nucleus (Supplementary Figure 1). We have used the same luciferase construct described before to study the effect of these peptides in the p53-PC4 interaction in the p53 mediated transactivation. As expected, PC4 in the presence of p53 could stimulate transactivation from pG13Luc promoters significantly while the activation was completely abolished by the wild-type peptide. However, almost no effect of the KKL 381, 382, 383 AAA-p53 (380-386) was observed, indicating specificity of the effect (Figure 4).

Serine-73 of PC4 plays an important role in p53-PC4 interaction

The PC4 protein consists of two functional domain of roughly equal size. The N-terminal half appears to be largely flexible and contains much of the regulatory post-translational modification sites. The C-terminal half binds to single stranded DNA and is also responsible for dimerization (Figure 5 (*A*)). The crystal structure of the C-terminal half of PC4 has recently been reported (23). We have attempted to elucidate the p53 interaction interface of PC4 by chemical shift perturbation using HSQC spectra. The HSQC spectra of PC4 has been assigned under low pH condition, previously (20). We have first attempted to obtain the HSQC spectra under more physiological conditions. At around the neutral pH, the spectra is not as well behaved but the pattern is very similar to the low pH spectra. One-to-one mapping of important resonances can be established and we have used this procedure to assign the spectra at around the neutral pH. Since it is

already known that the extreme C-terminal region of p53 is the most important interaction site, we have chosen p53 (380-386) for HSQC studies. Two versions of this peptide was used to obtain differential chemical shifts. One version of the peptide was acetylated at K381, K382 and K386, while the other contained three alanines at positions 381, 382 and 383. Advantage of using these peptides is that one binds with very high affinity and the other is at best a very weak binder, if at all. Overlap of the two HSQC spectra showed significant chemical shift changes for some resonances in the (Figure 5 (*B*)), but not for most. Only the distinctly resolved region is shown. Two of the most clearly identified resonances that show the largest shifts are Serine-73 and Glutamine-65. Since the cause of chemical shift perturbation could be due to direct interaction or indirect change in the environment due to interaction, we have mutated both these residues to find out their role in the p53 interaction. The GST pull-down assay, as described earlier, (15) was used to estimate the interaction strength of PC4S73A and PC4 Q65A (Figure 6 (*A*) and (B)) with p53 fusion protein. It is clear from the pull-down assay that S73A substitution affects the interaction significantly, whereas, Q65A mutation has little effect. This indicates that Serine-73 plays an important role in p53 interaction. This was confirmed by a fluorescence anisotropy assay (previously described) in which p53 (380-386) was fluorescein end-labeled and titrated with full-length PC4. The wild-type PC4 titration previously showed significant increase in fluorescence anisotropy indicating binding (Figure 2 (*C*)). However, for PC4S73A, no increase in fluorescence anisotropy was seen, indicating no significant binding in the concentration range studied (Figure 6 (*C*)).

The functional effects of S73A mutation in PC4 was tested in an *in vivo* gene expression activation assay using luciferase as the reporter gene in $p53^{-/-}$ H1299 cells. PG13Luc construct in which the luciferase gene is under the control of a promoter with 13 binding sites of p53 was used. PC4 in the presence of p53 could stimulate transactivation from pG13Luc promoter significantly (about 5 fold) as compared to transfection of p53 alone as reported earlier (Figure 6 (*D*), compare lane 2 versus lane 6). The vector control and PC4 alone showed negligible luciferase activity. Co-transfection of p53 with PC4Q65A was found to activate transcription from pG13Luc (about 4.8 fold as seen in Figure 6 (D); compare bar 2 versus bar 7) as compared to transfection of p53 alone, while, co-transfection of p53 with PC4S73A showed reduced transactivation (Figure 6 (D); compare bar 2 versus bar 8) from pG13Luc (about 2.4 fold).

PC4 directly interacts with p53 and enhances the DNA binding of p53 to its cognate sites. In order to investigate the functional significance of S73 mediated interaction of PC4 with p53, EMSA was performed using PC4S73A mutant and FLAG-tagged p53. The EMSA analysis showed that FLAG-p53 formed a sequence-specific complex, and as expected, the addition of wild type PC4 enhanced p53-mediated DNA binding in a dose-dependent manner (Figure 7 (*A*); lanes 3-6). In agreement with the results of the interaction studies, we found that PC4S73A mutant, which showed very weak interaction with p53, activated p53 DNA binding minimally (Figure 7 (*A*); lanes 3-6 versus lanes 7-10). The quantification of the EMSA data, indicated that at the concentration corresponding to 80 ng addition, wild type PC4 could enhance p53 DNA binding more than 2.5 fold as compared to the p53

interaction deficient point mutant PC4S73A (Figure 7 (*B*)).

The p53 region consisting of amino acids 380-386 may bind in the proximity of Serine-73. However, the mutagenesis experiments is not an unequivocal indication of the presence of the mutant residue in the binding site, as the mutation of a residue can exert a long-distance effect.

We have thus attempted to identify which residues may be present close to the bound 380-386 amino acid residues of p53 through intermolecular nuclear Overhauser effect. For this experiment, ^{15}N labeled PC4 was complexed with different acetylated p53 (380-386) peptide and edited 2D NOESY experiment was performed. In this experiment, only the NOEs from unlabeled protons to the protons attached to ^{15}N atoms are seen. We performed this experiment with ^{15}N-PC4 alone and in the presence of unlabeled triply acetylated p53 (380-386) as well as all the single acetylated peptides. Any additional NOE seen here is likely to originate from the peptide protons to the NH protons of PC4. We primarily focused on the acetyl peaks which are clearly distinguishable. We were able to clearly distinguish one NOE from acetyl group of lysine 381 to an amide proton (data not shown). To confirm this, we have synthesized the same peptide with deuterated acetyl group on lysine 381. Overlap of the protonated and deuterated K381Ac/^{15}N-PC4 complex, clearly shows an additional NOE from the protonated acetyl group to an amide group (Figure 8). Comparison of this NOE with HSQC done under identical conditions suggests that this residue is aspartate-76. This indicates presence of aspartate-76 in the binding pocket, close to lysine 381.

Discussion

Positive coactivator 4 or PC4 was originally isolated as a general transcription coactivator (9). Recent work suggests that it may play an important role in DNA repair and replication as well. A number of studies have pointed towards its important role in the activation of genes targeted by p53 (10). It is known to interact with p53 mainly through its C-terminal DNA binding domain (16). Apparently contradictory results have been reported about the location of the part of p53 that interacts with PC4. Initial reports suggest that PC4 interacts with both the C-terminal negative regulatory domain of p53 and the DNA binding domain and was supplemented by a recent report that it interacts with the N-terminal transactivation domain only (24). In this article, we have conclusively demonstrated binding of PC4 with 380-386 region of p53 which is modulated by acetylation of critical lysine residues (K382 and K381). The binding is at least two to three orders of magnitude stronger than the dissociation constant reported by Fersht and coworkers with full-length bacterially produced p53 (24). The high affinity for the 380-386 peptide reported here is consistent with conclusions of our previous work that major interaction with p53 occurs through the negative regulatory domain (16). Single point mutants obtained here and the functional assays with the single point mutants and chemical genetics approach with the p53 (380-386) peptide confirmed the role of negative regulatory domain's involvement in p53-PC4 interaction. It is not clear why bacterially produced full-length p53 did not bind with higher affinity, but could be due to differently folded nature of the full-length p53, when produced in *E.coli*.

NMR and mutagenesis experiments indicated that Serine-73 plays a crucial role in the interaction. Intermolecular NOE detected in 2D-NMR experiment suggested

that the K381 acetyl groups may be in close proximity with aspartate-76. Figure 9 shows the crystal structure of PC4 (bound to single stranded DNA) with the two residues highlighted. Both the residues are located in a trough away from the DNA binding region of PC4. This suggests that this region may bind p53 negative regulatory domain. The many-pronged approach reported here conclusively proves that wild-type p53-PC4 interaction occurs through the C-terminal regulatory region of p53. In a previous article, Banerjee et al., have demonstrated that p53Δ30 (p53 without the last 30 amino acids) retains most of the activation potential of PC4 (15). Those results seem to be apparently contradictory to the present results as well as other results consistent with the present results. Apart from the structural data, the peptide inhibition results presented here strongly suggests that the wild-type p53-PC4 interaction resulting in activation of gene expression occurs primarily through the residues 380-386 of p53. Batta *et al.,* had reported that the DNA binding domain of full-length p53 has weak PC4 interacting potential (16). The most likely explanation of activation by p53Δ30 is that in the full-length p53, the interaction with PC4 primarily occurs through the residues 380-386 and its deletion causes a conformational change in the DNA binding domain resulting in a stronger interaction with the interaction patch present in the DNA binding domain.

In the peptide model, acetylation of lysine-381 and 382, together led to an order of magnitude increase of affinity suggesting that acetylation may play a crucial role in the coactivation function of PC4. It has been previously established that acetylation of lysine-382 is crucial for full activation of p53 initiated pro-apoptotic transcription program (25,26). However, the mechanism of this acetylation dependence is not known. Significant enhancement of p53-PC4 interaction clearly provides a mechanism by which acetylation of lysine-382 modulates the p53 dependent target gene expression and pro-apoptotic response. However, this needs to be verified by direct experiments. Acetylation of PC4 by p300 has been shown to enhance double stranded DNA binding activity of PC4, resulting in enhanced activation function (16). Due to difficulty in obtaining single specifically acetylated p53, only plausible way at this time to understand the role of individual acetylations is through peptide models. However, information obtained from peptide models cannot readily be extended *a priori* to *in vivo* role of such post translational modifications and may only be thought of as indicative. However, peptide models employed to understand the post-translational modifications in N-terminal domain of p53 yielded a wealth of information which has largely been verified later (19).

If acetylation of K382 and K381 of p53 by p300 enhances the p53-PC4 interaction *in vivo* as suggested by peptide models, then activation of p300 may cause a synergistic activation of p53 targeted genes. In this study, it was demonstrated that peptide models could provide useful information regarding roles of post-translational modifications and show that PC4 could be an important partner in translating gene regulatory functions of p53.

References

1. Meek, D., and Anderson, C. (2009) *Cold Spring Harbor Perspectives in Biology* **1**, a000950. doi: 000910.001101/cshperspect.a000950.
2. Momand, J., Zambetti, G., Olson, D., George, D., and Levine, A. (1992) *Cell* **69**, 1237-1245
3. Dornan, D., Wertz, I., Shimizu, H., Arnott, D., Frantz, G., Dowd, P., O'Rourke, K., Koeppen, H., and Dixit, V. (2004) *Nature* **429**, 86-92
4. Leng, R., Lin, Y., Ma, W., Wu, H., Lemmers, B., Chung, S., Parant, J., Lozano, G., Hakem, R., and Benchimol, S. (2003) *Cell* **112**, 779-791
5. Haupt, Y., Maya, R., Kazaz, A., and Oren, M. (1997) *Nature* **387**, 296-299
6. Kubbutat, M., Jones, S., and Vousden, K. (1997) *Nature* **387**, 299-303
7. Oliner, J., Kinzler, K., Meltzer, P., George, D., and Vogelstein, B. (1992) *Nature* **358**, 80-83
8. Jayaraman, L., Moorthy, N., Murthy, K., Manley, J., Bustin, M., and Prives, C. (1998) *Genes & development* **12**, 462-472
9. Ge, H., and Roeder, R. (1994) *Cell* **78**, 513-523
10. Batta, K., Yokokawa, M., Takeyasu, K., and Kundu, T. (2009) *Journal of molecular biology* **385**, 788-799
11. Kaiser, K., Stelzer, G., and Meisterernst, M. (1995) *The EMBO journal* **14**, 3520-3527
12. Kretzschmar, M., Kaiser, K., Lottspeich, F., and Meisterernst, M. (1994) *Cell* **78**, 525-534
13. Das, C., Gadad, S., and Kundu, T. (2010) *J Mol Biol* **397**, 1-12
14. Das, C., Hizume, K., Batta, K., Kumar, B., Gadad, S., Ganguly, S., Lorain, S., Verreault, A., Sadhale, P., Takeyasu, K., and Kundu, T. K. (2006) *Molecular and cellular biology* **26**, 8303-8315
15. Banerjee, S., Kumar, B., and Kundu, T. (2004) *Molecular and cellular biology* **24**, 2052-2062
16. Batta, K., and Kundu, T. (2007) *Molecular and cellular biology* **27**, 7603-7614
17. Kumar, B., Swaminathan, V., Banerjee, S., and Kundu, T. (2001) *Journal of Biological Chemistry* **276**, 16804-16809
18. Kishore, A., Batta, K., Das, C., Agarwal, S., and Kundu, T. (2007) *The Biochemical Journal* **406**, 437-444
19. Sakaguchi, K., Saito, S., Higashimoto, Y., Roy, S., Anderson, C. W., and Appella, E. (2000) *J Biol Chem* **275**, 9278-9283
20. Jonker, H., Wechselberger, R., Pinkse, M., Kaptein, R., and Folkers, G. (2006) *FEBS Journal* **273**, 1430-1444
21. Fesik, S., Luly, J., Erickson, J., and Abad-Zapatero, C. (1988) *Biochemistry* **27**, 8297-8301
22. Arrowsmith, C. (1999) *Cell death and differentiation* **6**, 1169-1173
23. Werten, S., and Moras, D. (2006) *Nature structural & molecular biology* **13**, 181-182
24. Rajagopalan, S., Andreeva, A., Teufel, D., Freund, S., and Fersht, A. (2009) *Journal of Biological Chemistry* **284**, 21728-21737
25. Barlev, N., Liu, L., Chehab, N., Mansfield, K., Harris, K., Halazonetis, T., and Berger, S. (2001) *Molecular cell* **8**, 1243-1254
26. Roy, S., and Tenniswood, M. (2007) *J Biol Chem* **282**, 4765-4771
27. Polley, S., Guha, S., Roy, N., Kar, S., Sakaguchi, K., Chuman, Y., Swaminathan, V., Kundu, T., and Roy, S. (2008) *Journal of molecular biology* **376**, 8-12

Footnotes

Abbreviations: dsDNA: double stranded DNA; IPTG: b-isoproyl-thiogalactoside; MBHA: 4 – Methylbenzhydrylamine; HBTU: O-Benzotriazole-N,N,N',N'-tetramethyl-uronium-hexafluoro-phosphate; DMF: N,N-Dimethyl formamide; WATERGATE: Water suppression by Gradient-Tailored Excitation; EMSA: Electrophoretic Mobility shift assay; NOE: Nuclear Overhauser Effect; TOCSY: Total Correlation Spectroscopy

Acknowlegements: We acknowledge Department of Biotechnology, Government of India. We thank Dr. Selvi for technical as well as intellectual input. SR also acknowledges Council of Scientific and Industrial Research (India) and Department of Science and Technology, (Govt. Of India) for the J.C. Bose Fellowship.

Figure Legends

Figure *1*. (*A*) **Domain structure of p53**. (*B*) Overlap of methyl region TOCSY spectra of p53 (364-393) alone (blue) and p53 (364-393) in the presence of PC4 (10:1) (red). (*C*) Overlap of 1D spectra of methyl region of p53 (366-372) alone (blue) and p53 (366-372) in the presence of PC4 (7:1) (red). (*D*) Overlap of 1D spectra of methyl region of p53 (380-386) alone (blue) and p53 (380-386) in the presence of PC4 (7:1) (red). All the experiments were conducted at 37^{o}C on a 600-MHz Bruker Biospin NMR spectrometer using TCI cryoprobe. The buffer was 50 mM Potassium phosphate buffer, pH 6.2 containing 100 mM KCl. TOCSY (mixing time 60 ms) spectra were recorded with solvent suppression, which was achieved using WATERGATE and the spinlock in TOCSY experiment was attained by MLEV sequence. (*E*) GST pull-down assay: One microgram of GST (lane 2) or GST-p53 point mutant proteins (lanes 3 to 7) were incubated with bacterial lysate containing 200 ng of PC4 and analyzed by immunoblotting with anti-PC4 antibody. Lane 1, 20% input of bacterial cell lysate. Intensities relative to the GST only control are reported at the bottom.

Figure *2*. **Sedimentation velocity run of fluorescein end-labeled p53 (380-386).** (*A*) alone (SEDPHAT profile). *B*. Sedimentation velocity run of fluorescein end-labeled p53 (380-386) complex with PC4 (1:1). Scan was recorded at 495 nm. (*C*) Binding isotherm of fluorescein end-labeled p53 (380-386) with PC4 (solid diamond) and binding isotherm of fluorescein end-labeled p53 (380-386, KKL 381, 382, 383AAA) with PC4 (circles). (*D*) Effect of unlabeled p53 (380-386) (open circles) and p53 (380-386, KKL 381, 382, 383AAA) (solid circles) on Fluorescein labeled p53 (380-386)/PC4 complex. Fluorescence anisotropy measurements were performed at 4^{o}C by using a Quantamaster 6 (PTI) T-geometry fluorometer. The titrations were carried out in 20 mM Tris-HCl buffer, pH 7.4 containing 100 mM KCl, 0.2 mM EDTA, 20% glycerol and 0.1% NP40. Fluorescence anisotropy was measured with excitation at 490 nm and emission at 530 nm using bandwidths 5 nm. Further details are given in the Experimental Procedure.

Figure *3*. **Binding isotherms of acetylated p53 peptides**. Binding Isotherm of (Red) end-labeled p53 (380-386, K381Ac); (Green) end-labeled p53 (380-386, K382Ac); (Blue) end-labeled p53 (380-386, K386Ac) and (Black) end-labeled p53(380-386, KKK381, 382, 386 AcAcAc) with

PC4. Fluorescence anisotropy measurements were performed at 4°C by using Quantamaster 6 (PTI) T-geometry fluorometer. The titrations were carried out in 20 mM Tris-HCl buffer, pH 7.4 containing 100 mM KCl, 0.2 mM EDTA, 20% glycerol and 0.1% NP40. Fluorescence anisotropy was measured with excitation at 490 nm and emission at 530 nm using bandwidths 5 nm. The anisotropic data were fitted into a single site binding equation as described before (27).

Figure *4*. **Inhibition of PC4 enhancement of p53 activation of gene expression by p53 (380-386).** $p53^{-/-}$ H1299 cells were transfected with PG13-Luc (500ng), CMV-βGal (500ng), p53 (200 ng), PC4 (1.2 µg) in combinations as indicated. After 14 hours of transfection, WT peptide (WT) or control peptide (3A) were added in the indicated lanes. Following 24 hours of transfection, the luciferase activity was measured and normalized with β-galactosidase activity. Error bars show the standard errors of means of the replicates. +, present; -, absent.

Figure *5*. **Binding of acetylated p53 peptides by NMR**. (*A*) Cartoon drawing of modular structure of PC4. (*B*) Binding of PC4 and p53 (380-386) by NMR spectroscopy (^{1}H, ^{15}N HSQC). ^{1}H, ^{15}N HSQC overlaps of p53 (380-386, K381A,K382A,L383A)/ ^{15}N-PC4 (1:1) complex (blue) and p53 (380-386, K381KAc,K382KAc,K386KAc)/ ^{15}N-PC4 (1:1) complex (red). NMR experiments were conducted at 37°C on a 600-MHz Bruker Biospin NMR spectrometer using TCI cryoprobe. The buffer was 50 mM Potassium phosphate buffer, pH 6.2 containing 50 mM KCl and 50 mM d5 glycine.

Figure *6*. **Interaction of p53 (380-386) with mutant PC4**. (*A*) GST pull-down assay of p53 and mutant PC4 interaction: One microgram GST-p53 protein was incubated individually with bacterial lysate containing 200 ng of either PC4WT or PC4S73A, pulled down as described in the materials and methods and analyzed by immunoblotting with anti-PC4 antibody. Lanes 1 and 2 depicts 20% input of bacterial cell lysate containing PC4WT and PC4S73A, respectively. (*B*) One microgram GST-p53 protein was incubated individually with bacterial lysate containing 200 ng of either PC4WT or PC4Q65A, pulled-down and analyzed by immunoblotting with anti-PC4 antibody. Lane 1 and 2 depicts 20% input of bacterial cell lysate containing PC4WT and PC4Q65A respectively. (*C*) Binding isotherm of fluorescein end-labeled p53 (380-386) with PC4 S73A. Fluorescence anisotropy measurements were performed at 4°C by using Quantamaster 6 (PTI) T-geometry fluorometer. The titrations were carried out in 20 mM Tris-HCl buffer, pH 7.4 containing 100 mM KCl, 0.2 mM EDTA, 20% glycerol and 0.1% NP40. Fluorescence anisotropy was measured with excitation at 490 nm and emission at 530 nm using bandwidths 5 nm. (*D*) Gene expression activation by wild-type or mutant PC4: $p53^{-/-}$ H1299 cells were transfected with PG13-Luc (500ng), CMV-βGal (500ng), p53 (200ng), PC4WT (1.2µg), PC4Q65A (1.2µg) or PC4S73A (1.2µg) in combinations as indicated. Following 24 hours of transfection, the luciferase activity was measured and normalized with β-galactosidase activity. Error bars show the standard errors of means of the replicates. +, present; -, absent.

Figure *7*. **DNA binding by p53 in the presence of PC4**. (*A*) Three nanograms of a γ-^{32}P-labeled oligonucleotide containing a p53 binding site was incubated with 50 ng of p53 either in the absence of PC4 (lane 2) or with increasing concentrations of PC4 (lanes 3, 4, 5 and 6) or PC4S73A (lanes 7, 8, 9 and 10). Lane 1 contains the γ-^{32}P-labeled oligonucleotide alone. + present; - absent. (*B*) Quantitative representation of effect of PC4 and its point mutant S73A, on p53-mediated DNA binding. The levels of induction of p53-mediated binding are represented on

the *y* axis, and the increasing concentrations of PC4 or its point mutant PC4S73A on the *x* axis. Error bars are obtained from statistical analysis of multiple experiments.

Figure *8*. **Isotope-edited NOESY spectra**. Overlaps of isotope-edited NOESY spectra of p53 (380-386, K381Ac)/PC4 complex (1:1) (blue) and p53(380-386, K381KAc-d_3)/PC4 complex (1:1) (red). The upper spectra shows the ^{1}H, ^{15}N HSQC of p53 (380-386, K381Ac)-PC4 complex (1:1). Experiments were conducted at 37^{o}C on a 600-MHz Bruker Biospin NMR spectrometer using TCI cryoprobe. The buffer was 50 mM Potassium phosphate buffer, pH 6.2 containing 50 mM KCl and 50 mM d5 glycine.

Figure *9*. **Depiction of Space filling model of the C-terminal domain of PC4 (pdb id: 2C62)**. The two subunits are in grey and white. Following residues are highlighted: Serine-73 (blue); Aspartate-76 (red); Aspartate-84 (green) and glutamine-65 (cyan). The bound ssDNA is in wireframe model.

Table I

Sequence and nomenclature of peptides

NOMENCLATURE	SEQUENCE
p53(366-372)	SSHLKSK
p53(380-386)	HKKLMFK
p53(380-386, K381A, K382A, L383A)	HAAAMFK
p53(380-386, K381KAc)	HKAcKLMFK
p53(380-386, K382KAc)	HKKAcLMFK
p53(380-386, K386KAc)	HKKLMFKAc
p53(380-386, K381KAc, K382KAc, K386KAc)	HKAcKAcLMFKAc
6-D-Arg-NLS-p53(380-386, K381KAc,K382KAc, K386KAc)	$^{D}R_6$PKKKRKVHKAcKAcLMFKAc
6-D-Arg-NLS-p53(380-386)	$^{D}R_6$PKKKRKVHKKLMFK
6-D-Arg-NLS-p53(380-386, K381A, K382A, L383A)	$^{D}R_6$PKKKRKVHAAAMFK

Acetylated residues are highlighted in bold fonts, $^{D}R_6$ stands for 6-consecutive D-arginine residues, NLS stands for nuclear localization signal.

Figure 1 (A)

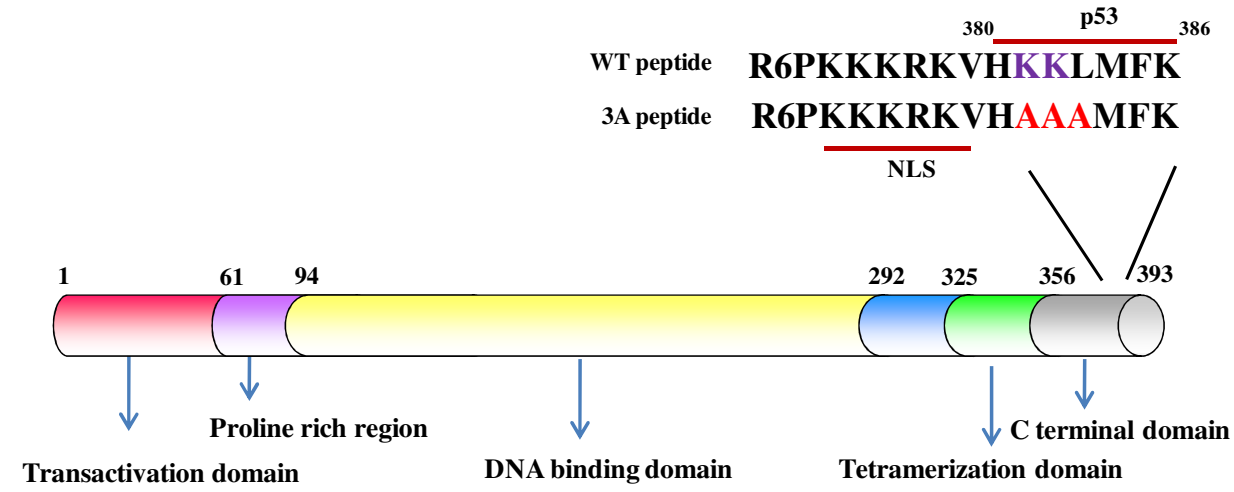

(B)

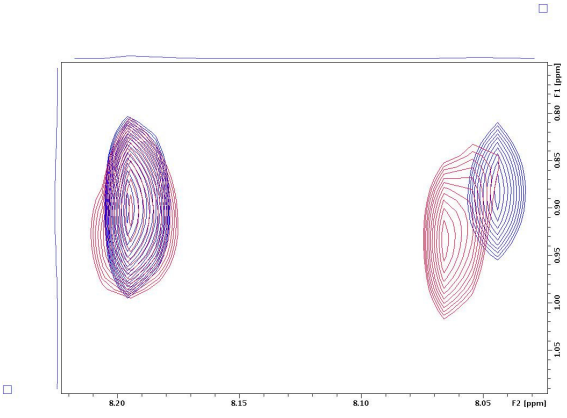

(D)

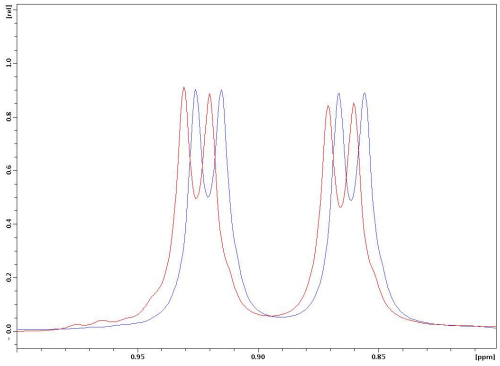

(C)

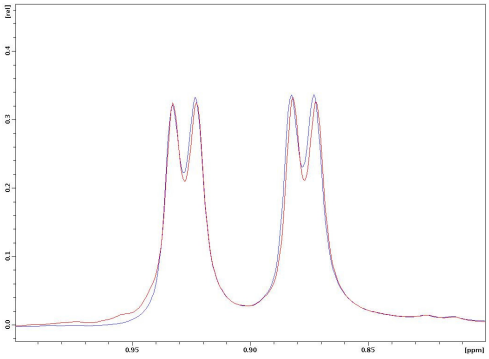

(E)

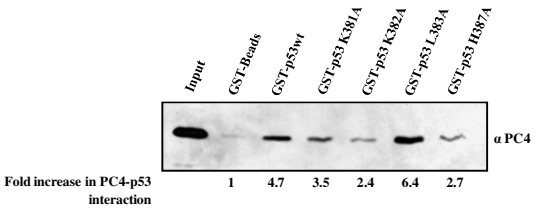

Figure 2

(A)

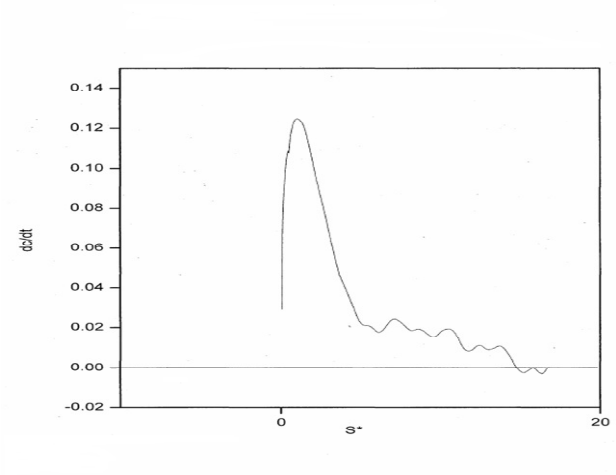

(B)

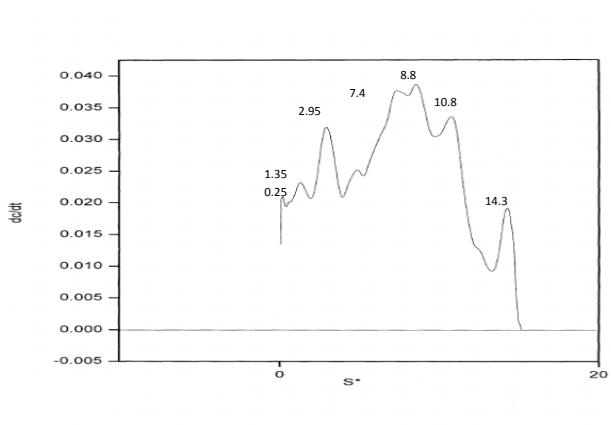

(C)

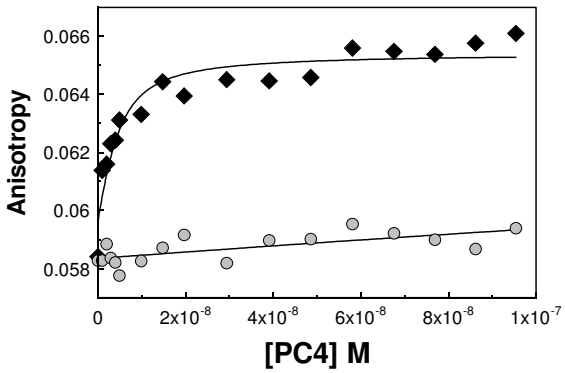

(D)

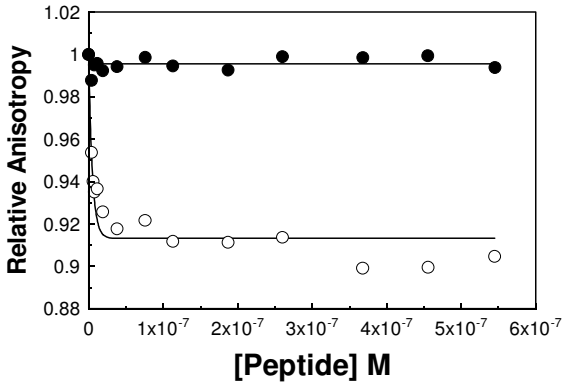

Figure 3

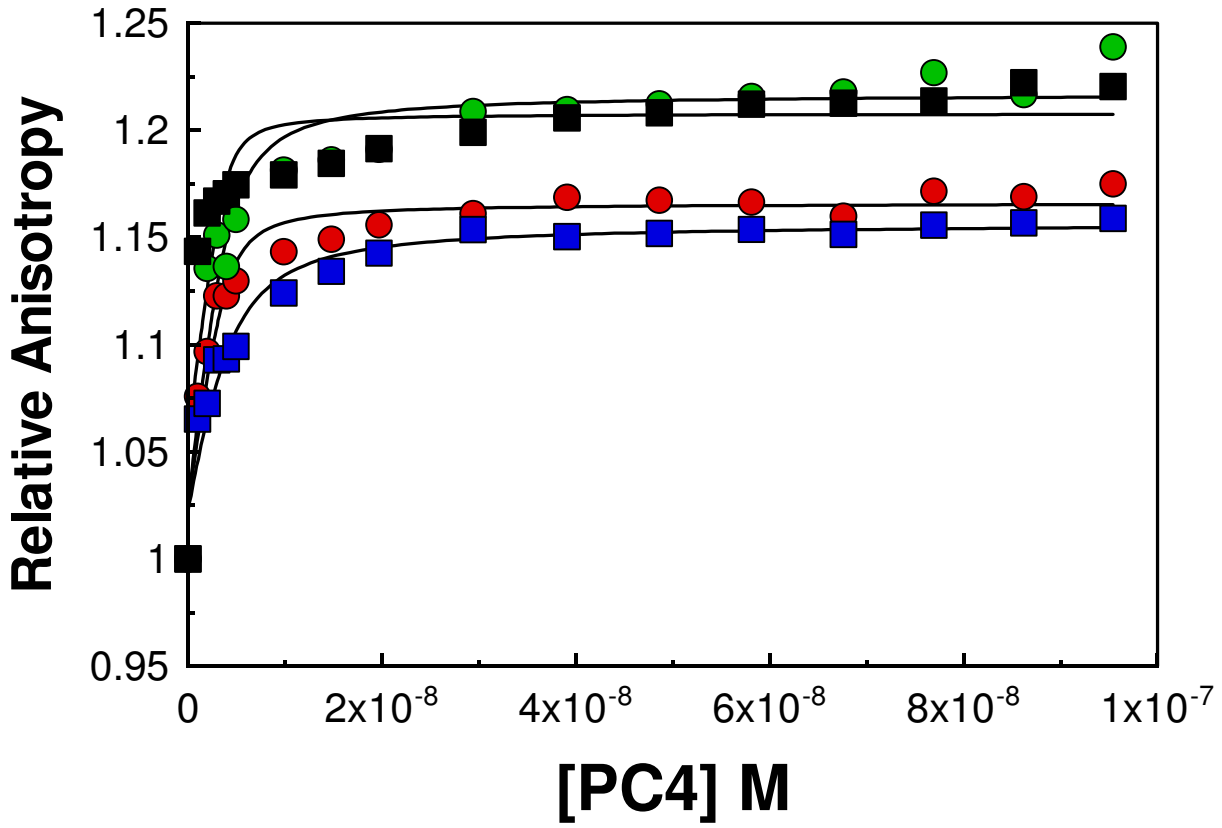

Figure 4

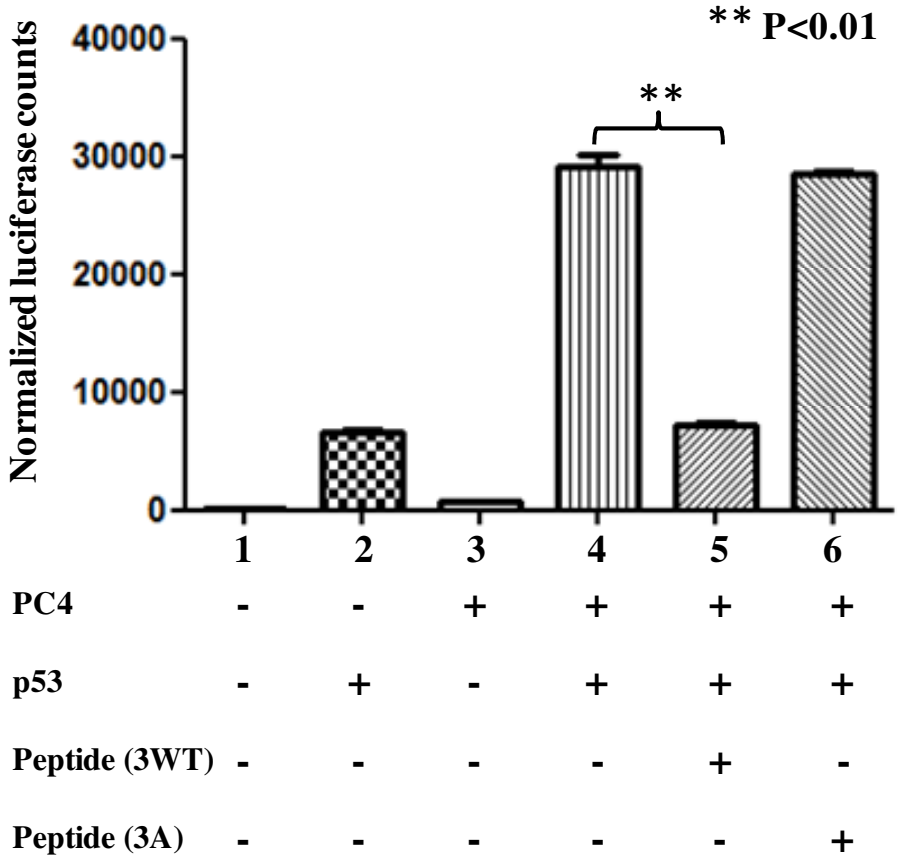

Figure 5

(A)

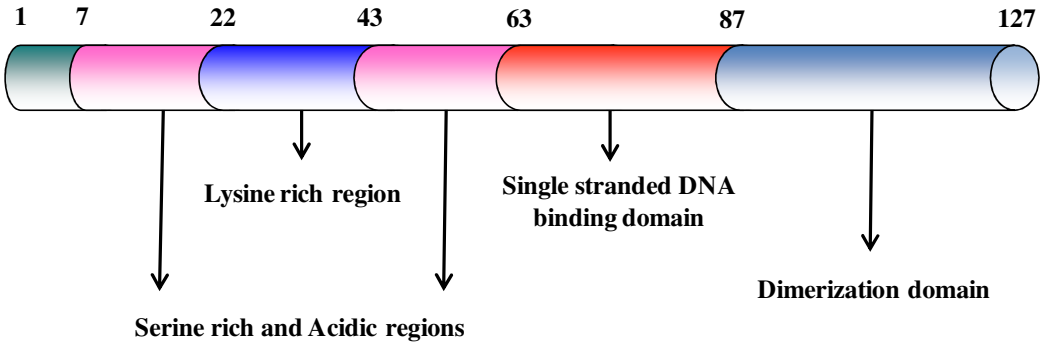

(B)

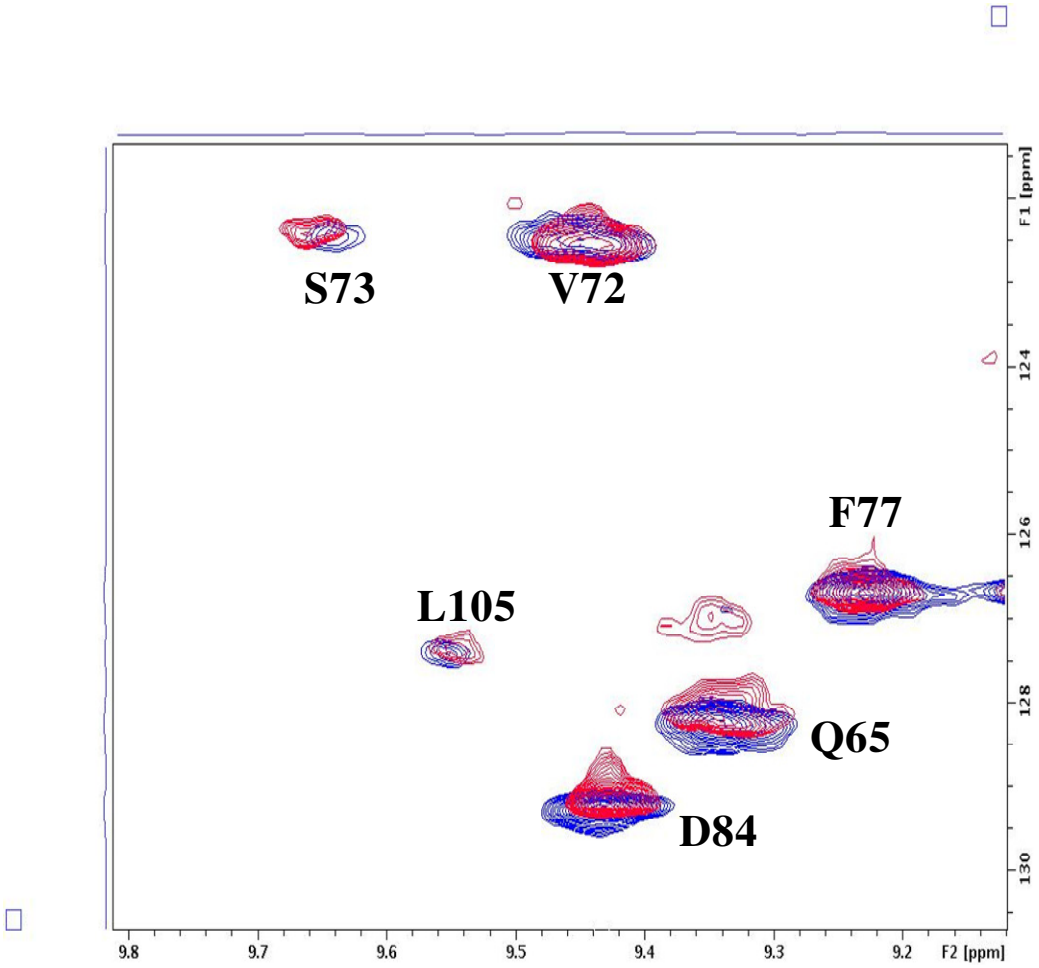

Figure 6

(A)

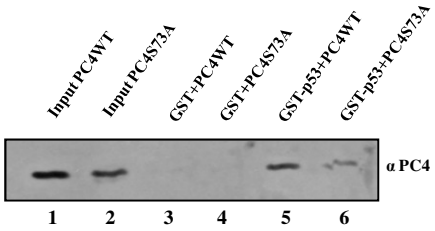

(B)

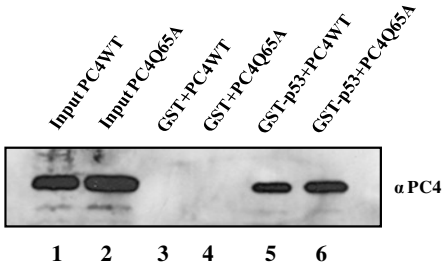

(C)

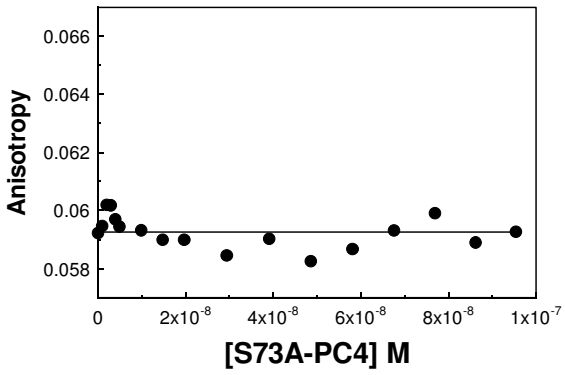

(D)

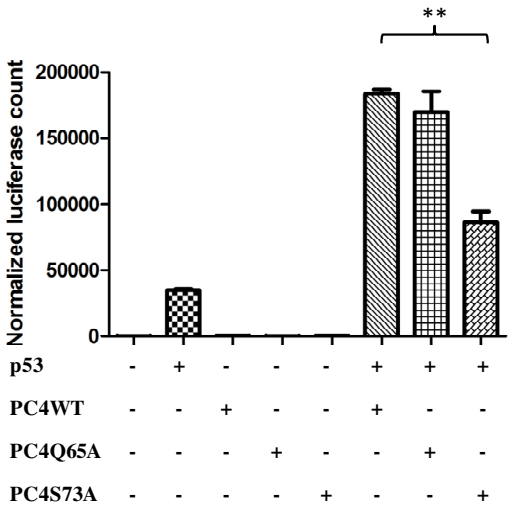

** P<0.01

Figure 7 (A)

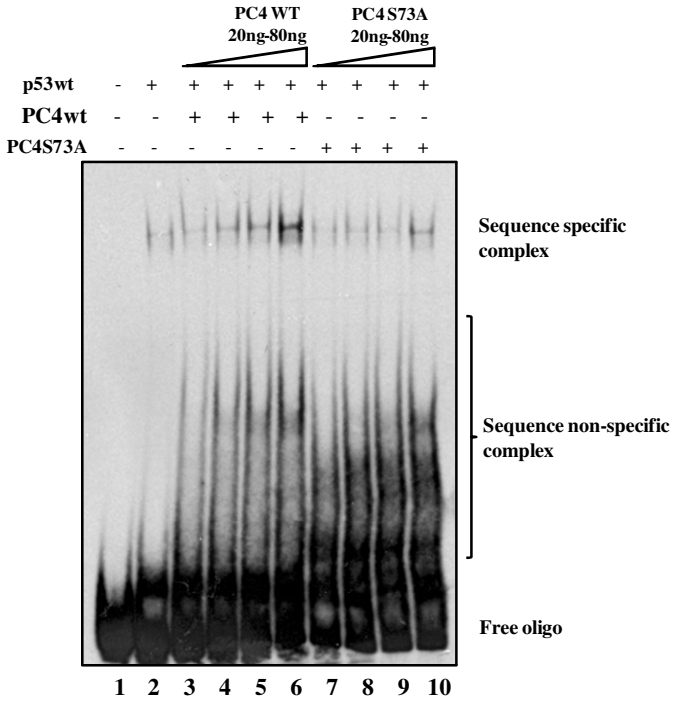

(B)

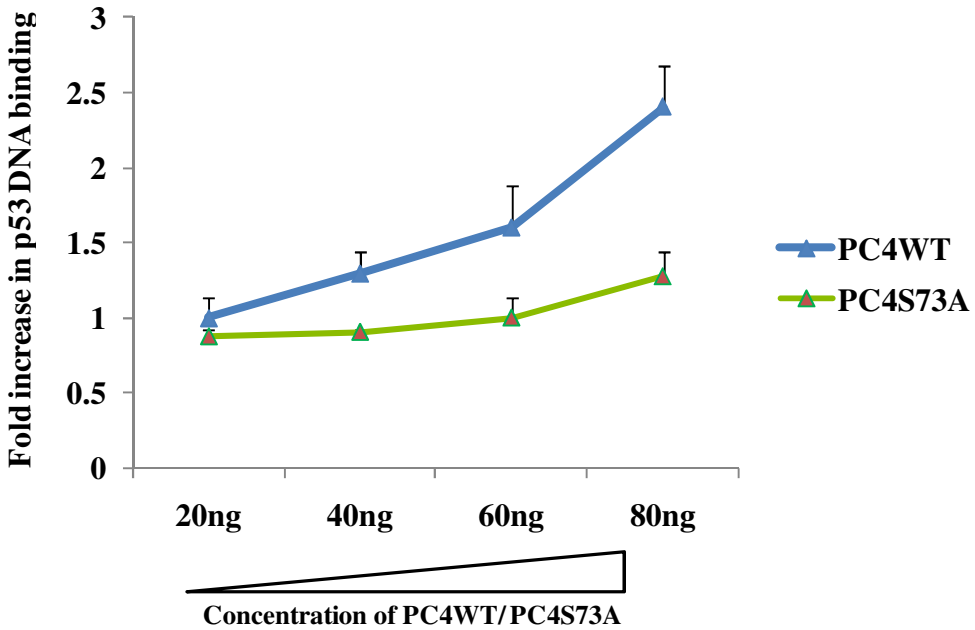

Figure 8

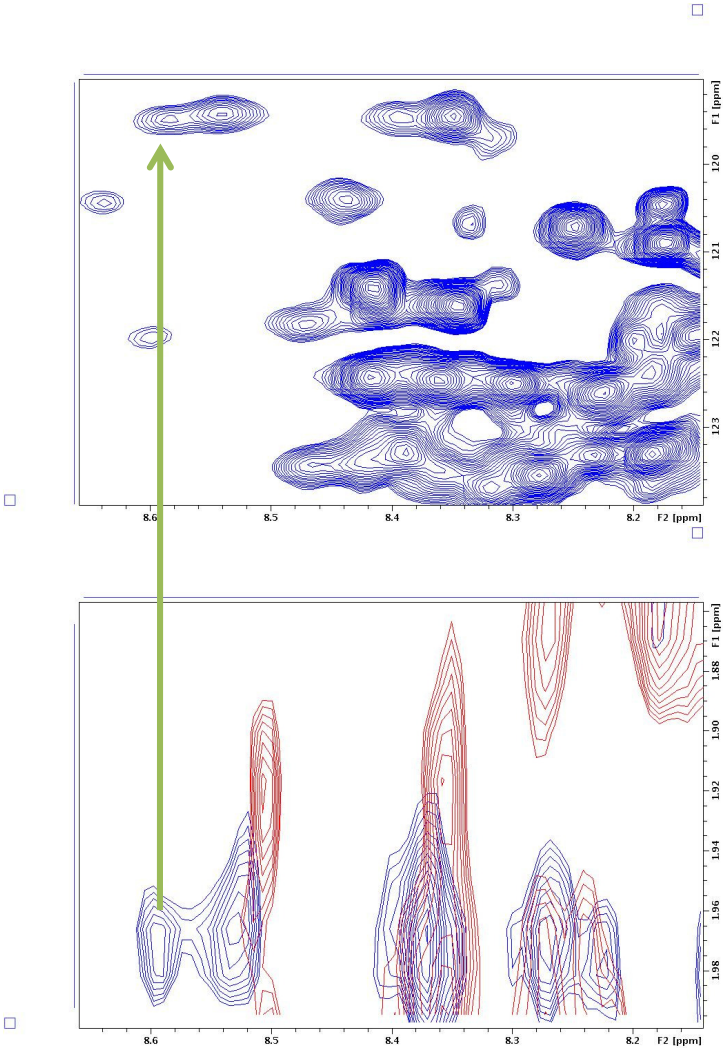

Figure 9